

Synthesis and characterization of CuInS₂ nanocrystalline semiconductor prepared by high-energy milling

Erika Dutková¹ · María J. Sayagués² · Jaroslav Briančin¹ · Anna Zorkovská¹ · Zdenka Bujňáková¹ · Jaroslav Kováč³ · Jaroslav Kováč Jr.³ · Peter Baláž¹ · Jana Ficeriová¹

Received: 2 September 2015 / Accepted: 14 October 2015 / Published online: 22 October 2015
© Springer Science+Business Media New York 2015

Abstract Nanocrystalline CuInS₂ particles have been synthesized from copper, indium, and sulfur powders by high-energy milling in a planetary mill in an argon atmosphere. Structural characterization of the prepared nanoparticles, including phase identification, Raman spectroscopy, specific surface area measurement, and particle size analysis were performed. The optical properties were studied using UV–Vis absorption and photoluminescence (PL) spectroscopy. The production of CuInS₂ (JCPDS 027-0159) particles with a crystallite size of about 17.5–23.5 nm was confirmed by X-ray diffraction. The crystal structure has a tetragonal body-centered symmetry belonging to the I-42d space group. The Raman spectra also proved the formation of pure CuInS₂ nanoparticles. TEM and HRTEM measurements revealed the presence of nanoparticles of different dimensions (10–20 nm) and their tendency to form agglomerates. The nanoparticles tend to agglomerate due to their large specific surface area. The average size of the synthesized particles was determined by photon cross-correlation spectroscopy to be in the range of 330–530 nm (bimodal size distribution). The band gap of the CuInS₂ particles is 2 eV which is wider than that in bulk materials. The decrease in size leads to the blue-shift of the PL spectra. Therefore, CuInS₂ nanoparticles are

promising candidates for optical applications, and they have high potential in solar energy conversion.

Introduction

Ternary semiconductors of the I–III–VI₂ group have received considerable attention over the last decades due to their potential technological applications such as photoelectrochemical cells, photoconductivity characteristics, and other beneficial intrinsic properties. They are actively used in the optoelectronic and solar cell applications [1–4]. However, many of the best studied nanocrystalline materials contain toxic heavy metals; this seriously limits their potential for widespread application. Copper indium disulfide CuInS₂ is a selenium-free compound from the chalcopyrite family, and its development is attractive because the problematic selenium is substituted by non-toxic sulfur in this case. Bulk CuInS₂ is a semiconductor with a direct optical band gap of 1.5 eV (820 nm) and with high absorption coefficient of the order of 10⁵ cm⁻¹ [5].

Among different materials, CuInS₂ may be a promising semiconductor material due to its applications in the area of visible and infrared light-emitting diodes, solar cells, infrared detectors, optical parametric oscillators, upconverters, far-infrared generators, etc. [6–9]. There are various techniques [10–18] for the synthesis of CuInS₂ powders and thin films with different nano- and micro-forms, such as nanoparticles [12], nanorods [14], porous microspheres [15], nanotubes [16], foam-like nanocrystallites [17], and nanowires [18], including chemical vapor deposition (CVD), solvothermal route, spray pyrolysis, vacuum evaporation, sputtering, and thermal evaporation.

Mechanochemistry offers new challenges in the synthesis of nanocrystals [19, 20]. This synthetic route can be

✉ Erika Dutková
dutkova@saske.sk

¹ Institute of Geotechnics, Slovak Academy of Sciences, Watsonova 45, 04001 Kosice, Slovakia

² Institute of Material Science of Seville (CSIC-US), 410 92 Seville, Spain

³ Institute of Electronics and Photonics, Slovak University of Technology and International Laser Centre, 81219 Bratislava, Slovakia

performed via simple solid-state approach using ambient pressure and room temperature.

This paper is focused on the synthesis and study of structural, surface, and optical properties of mechanochemically synthesized CuInS₂ nanoparticles from the point of view of the possible application. The controlled mechanochemical synthesis of nanocrystalline CuInS₂ at ambient temperature in the absence of a solvent is still a great challenge.

Experimental

Mechanochemical synthesis of CuInS₂ was performed in a planetary ball mill (Pulverisette 6, Fritsch, Germany) starting from powders of copper (99.7 %, Aldrich, Germany), indium (99.99 %, Aldrich, Germany), and sulfur (99 %, Ites, Slovakia) in an argon atmosphere, according to the reaction:



The milling was performed in a 250-ml tungsten carbide milling chamber with 50 tungsten carbide balls, 10 mm in diameter. The rotational speed of the planet carrier was 550 rpm. The powder charge was 1.31 g Cu, 2.37 g In, and 1.32 g S, corresponding to the stoichiometry of Eq. (1). The milling time was 30–120 min and the mill operated at room temperature.

The X-ray diffraction patterns were obtained using a D8 Advance diffractometer (Bruker, Germany) in the Bragg–Brentano geometry, working with a CuK_α radiation and a scintillation detector. For the data treatment, the commercial Bruker processing tools have been used. Specifically, for phase identification the Diffrac^{plus} Eva and for Rietveld analysis the Diffrac^{plus}Topas software have been utilized.

The micro-Raman measurements were performed in air at room temperature, with the focus of the beam of an Ar laser (514 nm) via a confocal Raman Microscope (Spectroscopy & Imaging, Germany) in backscattering geometry. The frequency of the Raman line of crystalline Si at 520 cm⁻¹ was used to calibrate the system in the present study.

The specific surface area was determined by the low-temperature nitrogen adsorption method in a Gemini 2360 sorption apparatus (Micromeritics, USA).

The particle size distribution was measured by photon cross-correlation spectroscopy (PCCS) using a Nanophox particle size analyzer (Sympatec, Germany). A part of the sample was added into distilled water and sonicated for 10 min. Then the sample was further diluted, in order to achieve a suitable concentration for the measurement by PCCS. The analyses were performed with a dispersant refractive index of 1.33 and in the range 10–10,000 nm.

The measurements were performed 3 times for each sample.

The morphology and microcharacterization of the sample were analyzed using scanning electron microscopy (SEM) and transmission electron microscopy (TEM) techniques. A small quantity of the powder sample was deposited on carbon-coated copper grids (for SEM) or nickel grids (for TEM, to avoid the interference between the Cu grid and the Cu from the sample in the EDS analysis). A MIRA3 FE-SEM microscope (TESCAN, Czech Republic) equipped with EDX detector (Oxford Instrument, United Kingdom) was used. The sample was sufficiently conductive, thus it is not coated with any conductive material in order to avoid charging artifacts. An FEI TECNAI G2 F30 S-twin high-resolution transmission electron microscope (HRTEM) was used, with field emission gun (FEG) and scanning transmission capabilities (STEM) operating at 300 kV and 0.2 nm point resolution, equipped with a high-angle annular dark-field (HAADF) detector with 0.16 nm point resolution from Fischione Instruments, and an INCA X-Max 80 silicon drift detector (SDD) for the energy-dispersive X-ray analysis (EDX). The Gatan Digital Micrograph software (Gatan Inc.) was used to measure the lattice spacing and to calculate the First Fourier Transform (FFT). The analysis of the HAADF-STEM images and the EDX profile was done with the ES Vision software (FEI Company).

The absorption spectra were measured using an UV–Vis spectrophotometer Helios Gamma (Thermo Electron Corporation, Great Britain) in quartz cell by dispersion of the synthesized particles in absolute ethanol by ultrasonic stirring.

The micro-PL spectra were measured by an UV–Vis–NIR confocal Raman Microscope (Spectroscopy & Imaging, Germany). The excitation at 514 nm was carried out using an Ar laser. For measuring the PL intensity, the nanopowders were dispersed on SiO₂/Si substrate.

Results and discussion

The progress of the mechanochemical synthesis of CuInS₂ is illustrated by XRD patterns of samples taken after 30–120 min of milling (a–c) (Fig. 1). The mechanochemical reaction is completed after 30 min of milling. The product was identified via XRD analysis as roquesite (JCPDS 027-0159). The crystal structure has a tetragonal body-centered symmetry belonging to the I-42d space group with the lattice parameters $a = b = 5.523 \text{ \AA}$ and $c = 11.141 \text{ \AA}$. The characteristic peaks of other impurities were not detected. The most intense peak appeared at 27.9° is attributed to the chalcopyrite phase oriented along the [112] crystal plane. The estimated average crystallite size

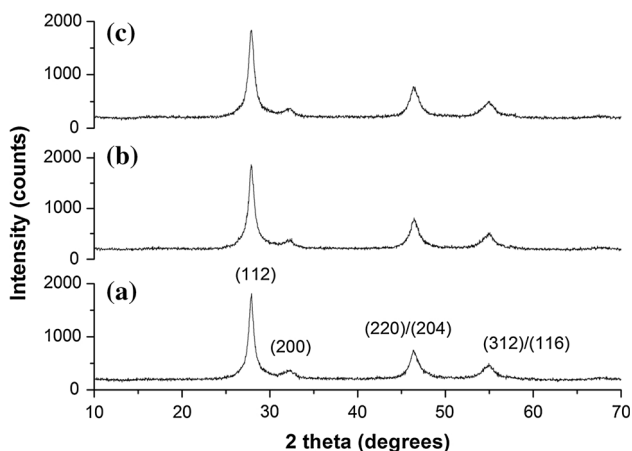


Fig. 1 XRD patterns of the mechanochemically synthesized CuInS₂ nanoparticles after **a** 30 min, **b** 60 min, and **c** 120 min of milling

is 23.5 nm for the CuInS₂ milled for 30 min. Milling for 60 min leads to obvious but not too dramatic structural refinement, and the crystallite size decreases to 18 nm. No considerable changes can be observed after milling for 120 min (crystallite size is 17.5 nm).

Raman spectroscopy confirmed the pure crystalline nanoparticle formation. In Fig. 2, the micro-Raman spectra of the synthesized sample are given. The figure shows that the dominant features of Raman plots are intense peaks at 298 cm⁻¹ and the weaker peaks at 240 and 340 cm⁻¹, which were previously assigned to the A₁, E, and B₂ modes of CuInS₂ phase, respectively [9, 21]. No other Raman peaks were observed, indicating pure CuInS₂ nanoparticle growth. It can be also seen that at 40 % excitation power recrystallization of the structure occurs, manifested by increase and narrowing of the peak at 298 cm⁻¹ and decrease of the other peaks in comparison

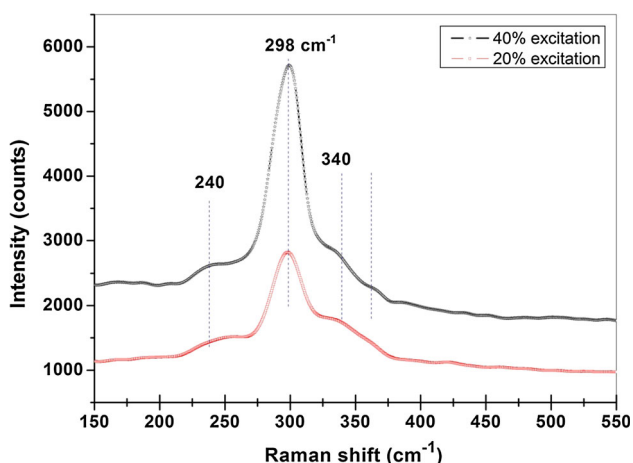


Fig. 2 Micro-Raman spectra of the mechanochemically synthesized CuInS₂ during 60 min. The wavelength of the incident laser light was 514 nm

with the Raman spectra measured at only 20 % excitation power by laser light.

The high-energy milling of solids is accompanied by an increase in the number of nanoparticles and by generation of fresh, previously unexposed surface. Specific surface area values belong to one of the most important characteristics of the milled samples [19]. The specific surface area of the mechanochemically synthesized CuInS₂ nanoparticles was in the range 3.4–4.0 m² g⁻¹. Particles in the nanometer size range have a strong tendency to agglomerate due to their relatively large specific surface area.

The particle size distribution of the nanocrystalline CuInS₂ nanoparticles was characterized using a photon cross-correlation spectroscopy as shown in Fig. 3. The size dispersion has a relatively narrow, bimodal distribution profile, with an average particle size in the range of 250–670 nm, indicating that relatively large agglomerates of CuInS₂ resulted from high-energy ball milling.

The surface morphology of the mechanochemically synthesized CuInS₂ was pursued using SEM. The micrographs are presented in Fig. 4.

As can be seen from the microscopic point of view (left part of Fig. 4a), the tendency toward agglomeration is evident. After 60 min of milling, together with the presence of larger grains, also very fine grains occur. Very fine particles can be observed, and although agglomerates are formed, these fine particles belonging to nano-region are retained. To confirm the presence of nanoparticles definitely, even higher magnification was used (Fig. 4b). It can be concluded that the CuInS₂ sample exhibits agglomerated grains with large amount of nanoparticles. From SEM images, it is also evident that particles are clusters of tiny crystallites.

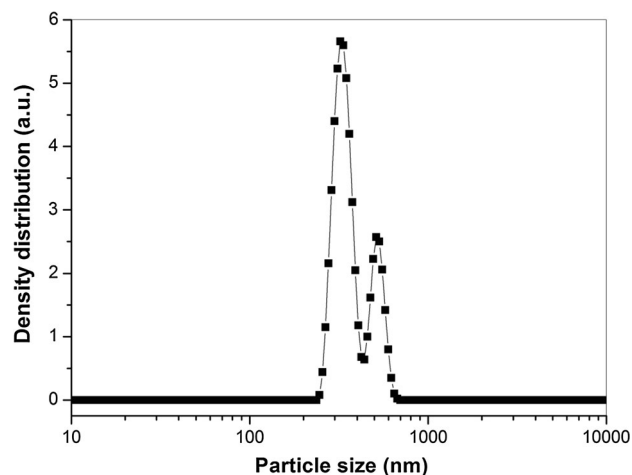


Fig. 3 Particle size distribution of the mechanochemically synthesized CuInS₂ during 60 min

Fig. 4 SEM images with lower (*left*) and higher (*right*) magnification of the mechanochemically synthesized CuInS₂ during 60 min. (*scale bars left*—1 μm, *right*—200 nm)

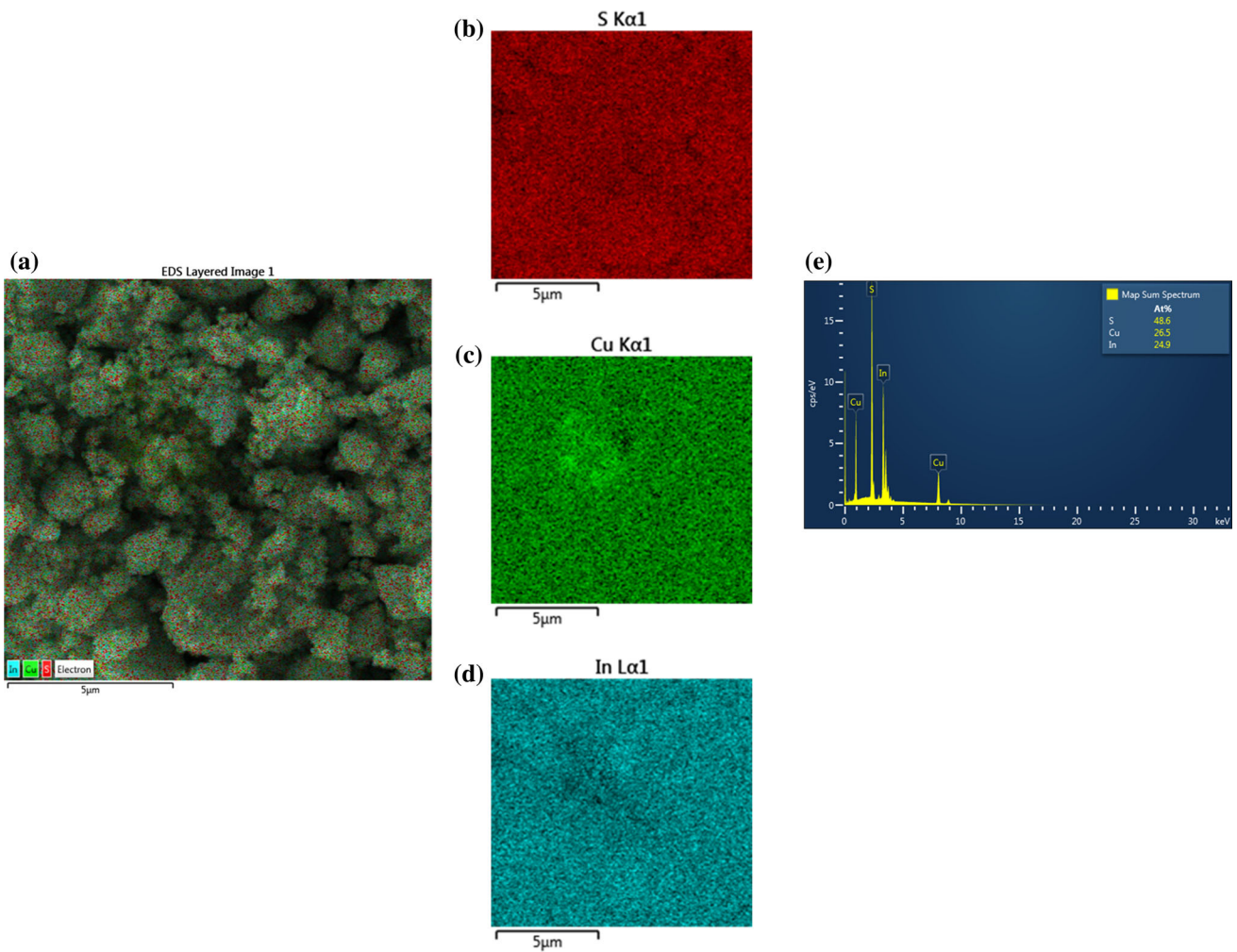
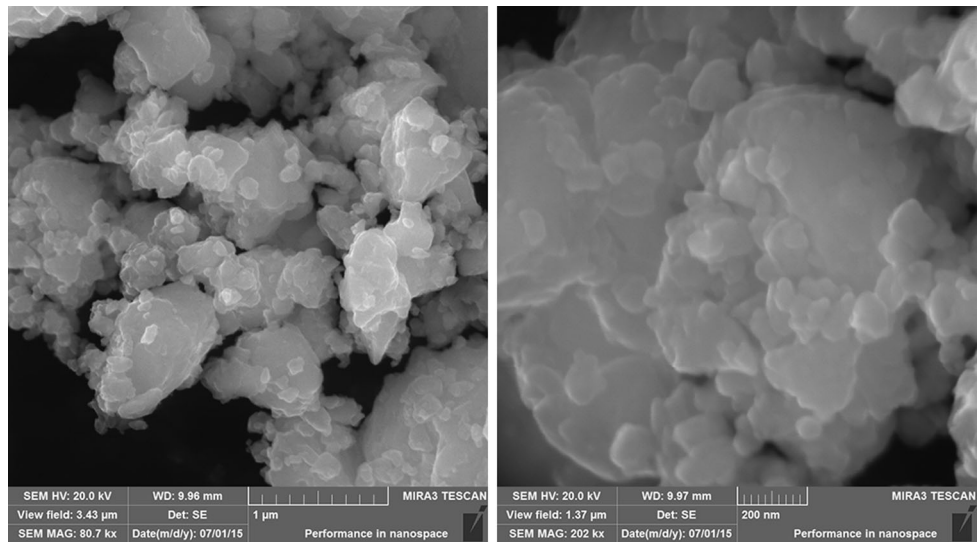
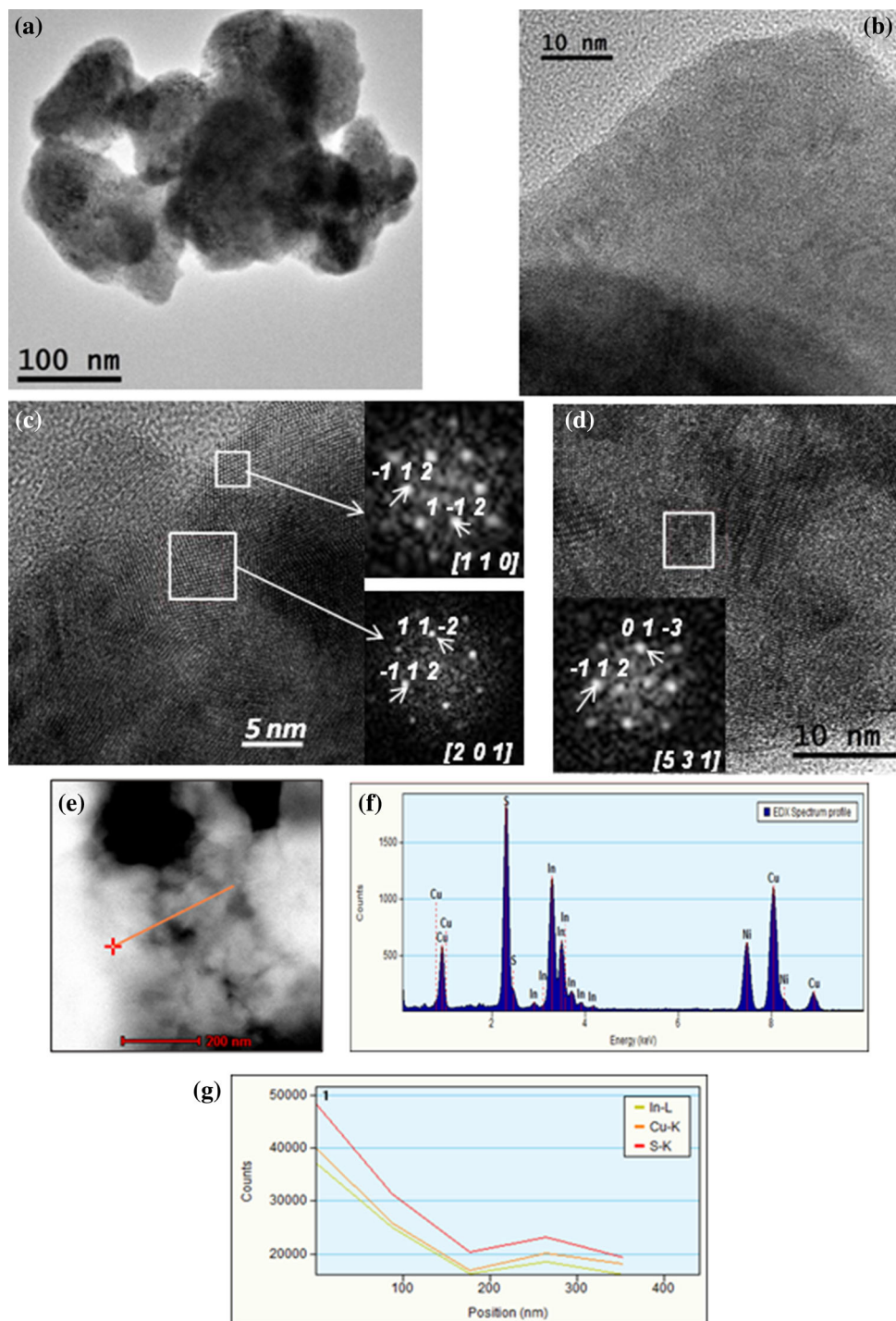


Fig. 5 **a** EDS layered image, **b** EDS map of S distribution, **c** EDS map of Cu distribution, **d** EDS map of In distribution, and **e** EDX spectrum

Fig. 6 Microcharacterization of CuInS_2 sample synthesized mechanochemically during 60 min. **a** TEM image; **b–d** HRTEM micrographs; **e** HAADF-STEM image, the line profile analysis is marked with a red line; **f** EDX spectrum taken in the first dot of the scanning image. **g** Representation of the Cu–In–S EDS signal in each point of the line profile



The EDS layered image comprising all the elements is illustrated in Fig. 5a. The energy-dispersive X-ray spectroscopy (EDS) elemental mapping for the mechanochemically synthesized CuInS_2 is shown in Fig. 5b–d. It can be clearly seen that all constituent elements are uniformly distributed over the as-prepared sample confirming the homogeneity of the powder. In the EDX spectra (Fig. 5e), the same elements can be observed.

The results confirm the presence of the elements from which the mechanochemically synthesized CuInS_2 is formed and a significant amount of copper (26.5 at.%), indium (24.9 at.%), and sulfur (48.6 at.%) is evidenced. However, it has to be noted that synthesized product is of the desired purity.

The microstructure of the CuInS_2 sample after 60 min of milling was further studied using TEM, HRTEM, EDS, and

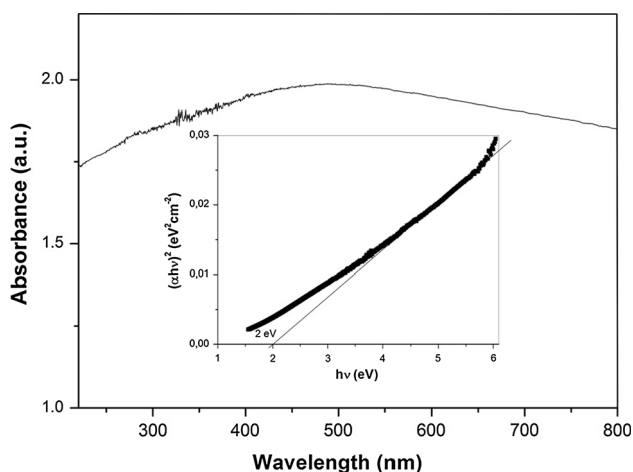


Fig. 7 UV-Vis spectrum of the mechanochemically synthesized CuInS₂ during 60 min. The inset shows the plot of $(\alpha hv)^2$ versus $h\nu$ curve

HAADF-STEM techniques, and the obtained results are depicted in Fig. 6. In the TEM image (Fig. 7a), it was found that the sample is formed by quite large particles (100–300 nm), and this result is in good agreement with that determined by photon cross-correlation spectroscopy. However, the HRTEM images show that those particles are formed by agglomerated nanocrystals of CuInS₂ with very small crystallite size (10–20 nm), confirming the results of XRD analysis.

In some particle edges, the initial crystallization and some amorphous areas can be observed (Fig. 6b). Some oriented nanocrystals were elucidated from the contrast (marked with a white square) in the images presented in Fig. 6c, d, and the first Fourier transform (FFT) was done to estimate the zone axis of the orientation. The results show the [110], [201], and [531] zone axes of the tetragonal roquesite system. The Cu, In, and S atomic percentages were analyzed by EDX technique in the STEM mode with an HAADF detector. A line profile analysis was done through the red line marked in the HAADF-STEM image (Fig. 6e) and five dots were analyzed. The EDX spectrum taken in the first point is depicted in Fig. 6f and the S–K, Cu–K, L, and In–L edges are well observed. A resume of the S–Cu–In signal through the line profile is represented in Fig. 6g.

As the size of the nanoparticles decreases, the band gap increases and the absorption and photoluminescence spectra shift to shorter wavelengths. Figure 7 shows the optical absorption properties of the mechanochemically synthesized (60 min) CuInS₂ investigated by UV-Vis spectroscopy. The band gap of the CuInS₂ is approximated using the direct band method, by plotting the squared absorbance versus energy and extrapolating to zero, as shown in the inset. The band gap of CuInS₂ is estimated to be 2.0 eV, which is in good agreement with the previous reports [12, 22, 23]. The observed peak is blue-shifted

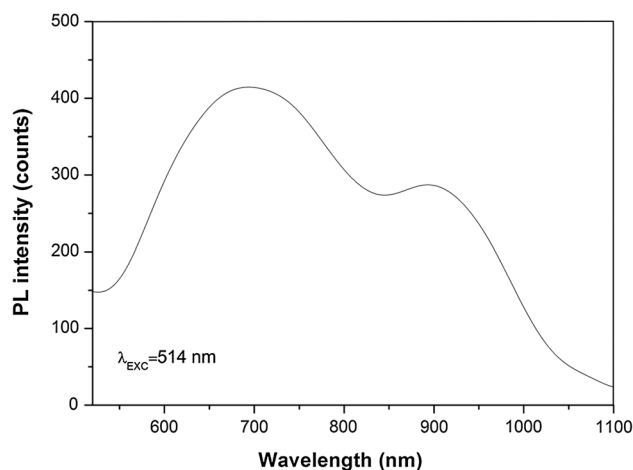


Fig. 8 PL spectrum of the mechanochemically synthesized CuInS₂ during 60 min

relative to the bulk CuInS₂ at 1.5 eV [5] and is assigned to the optical transitions of the excitonic states in CuInS₂. The obvious blue-shift could be attributed to the existence of very small CuInS₂ nanocrystalline particles agglomerated into the large clusters.

The micro-PL spectrum of the mechanochemically synthesized nanocrystallites is shown in Fig. 8. With the excitation wavelength at 514 nm, the corresponding emission peaks were found at around 700 nm (1.77 eV) and 900 nm (1.37 eV). The peak observed at 700 nm is in accordance with the literature [24]. The broad PL emissions are typically observed in chalcopyrite I–III–VI₂-based semiconductor nanocrystals. The radiative recombination of excited electron–hole pairs in such nanocrystals is associated with deep defect states inside the band gap, being referred to as donor–acceptor pair recombination [5]. Probably, the peak at 900 nm (1.37 eV) may be attributed to a transition from shallow trap centers to the conduction band [25].

As can be seen (Figs. 7, 8), the decreasing size of CuInS₂ leads to the blue-shift of the absorption and PL spectra. In addition, the PL spectrum is red-shifted compared to the absorption spectrum, which indicates the large Stokes shift of the nanoparticles.

Conclusion

Nanocrystalline copper indium disulfide CuInS₂ has been synthesized by high-energy ball milling in a planetary mill in an argon atmosphere. The obtained material had a tetragonal crystalline structure. TEM measurements also revealed the presence of nanocrystals with the size of 10–20 nm with the tendency to form agglomerates. The bimodal size distribution profile was found with a mean particle size in the range of

330–530 nm. Using the SEM microscopy, elemental mapping proved the homogeneous distribution of Cu, In, and S elements. Both UV–Vis absorption and PL emission spectra recorded for CuInS₂ indicate quantum size effects. Such prepared nanocrystalline CuInS₂ has a wider band gap (2 eV) in comparison to the bulk one (1.5 eV) what could be in many aspects of application more beneficial. Mechanochemical synthesis of nanocrystalline ternary metal chalcogenides may be a contribution to nanotechnology and materials engineering. The controlled mechanochemical synthesis can be considered environmentally friendly, because a solvent-free mechanochemical procedure was performed under ambient temperature and atmospheric pressure.

Acknowledgements The support through the Slovak Grant Agency VEGA (projects 2/0027/14, 1/0439/13, 2/0051/14) and APVV 14-0103 is gratefully acknowledged. The authors also acknowledge the support of the European Union through the CT-2011-1-REG-POT285895 AL-NANOFUN project (Advanced Laboratory for the Nano-Analysis of novel Functional materials), for the microscopy facilities sited at the Institute of Materials Science in Seville.

References

- Green MA, Emery K, King DL, Igari S, Warta W (2002) Solar cell efficiency tables (version 20). *Prog Photovolt* 10(5):355–360. doi:10.1002/Pip.453
- Pinjari DV, Pandit AB (2010) Cavitation milling of natural cellulose to nanofibrils. *Ultrason Sonochem* 17(5):845–852. doi:10.1016/j.ultsonch.2010.03.005
- Klenk R, Klaer J, Scheer R, Lux-Steiner MC, Luck I, Meyer N, Rühle U (2005) Solar cells based on CuInS₂—an overview. *Thin Solid Films* 480:509–514. doi:10.1016/j.tsf.2004.11.042
- Kazmerski L, Ramanathan K (2005) The 14th international conference on ternary and multinary compounds. *J Phys Chem Solids* 66(11):1853. doi:10.1016/j.jpcs.2005.10.171
- Xiao JP, Xie Y, Tang R, Qian YT (2001) Synthesis and characterization of ternary CuInS₂ nanorods via a hydrothermal route. *J Solid State Chem* 161(2):179–183. doi:10.1006/jssc.2001.9247
- Zhou JC, Li SW, Gong XL, Yang YL, Guo Y (2011) Preparation of CuInS₂ microspheres via a facile solution-chemical method. *Mater Lett* 65(12):2001–2003. doi:10.1016/j.matlet.2011.03.089
- Kim KH, Lee JK, Alphonse A, Erkan ME, Shin DC, Lim DG, Park BO, Jin MHC (2013) Preparation of precursor particles by cryogenic mechanical milling for the deposition of CuInS₂ thin films. *Mater Sci Semicond Process* 16(1):226–230. doi:10.1016/j.mssp.2012.08.012
- Amiri O, Salavati-Niasari M, Sabet M, Ghanbari D (2013) Synthesis and characterization of CuInS₂ microsphere under controlled reaction conditions and its application in low-cost solar cells. *Mater Sci Semicond Process* 16(6):1485–1494. doi:10.1016/j.mssp.2013.04.026
- Li DS, Zou Y, Yang DR (2012) Controlled synthesis of luminescent CuInS₂ nanocrystals and their optical properties. *J Lumin* 132(2):313–317. doi:10.1016/j.jlumin.2011.08.030
- Scheer R, Klenk R, Klaer J, Luck I (2004) CuInS₂ based thin film photovoltaics. *Sol Energy* 77(6):777–784. doi:10.1016/j.solener.2004.08.004
- Long F, Wang WM, Tao HC, Jia TK, Li XM, Zou ZG, Fu ZY (2010) Solvothermal synthesis, nanocrystal print and photoelectrochemical properties of CuInS₂ thin film. *Mater Lett* 64(2):195–198. doi:10.1016/j.matlet.2009.10.044
- Han SK, Kong MG, Guo Y, Wang MT (2009) Synthesis of copper indium sulfide nanoparticles by solvothermal method. *Mater Lett* 63(13–14):1192–1194. doi:10.1016/j.matlet.2009.02.032
- Lee DY, Kim J (2010) Characterization of sprayed CuInS₂ films by XRD and Raman spectroscopy measurements. *Thin Solid Films* 518(22):6537–6541. doi:10.1016/j.tsf.2010.03.062
- Jiang Y, Li Q, Chen J (2014) Synthesis and characterization of chalcopyrite CuInS₂ nanorods by an organic molten salt method. *Mater Lett* 120:182–184. doi:10.1016/j.matlet.2014.01.079
- Hu HM, Yang BJ, Liu XY, Zhang R, Qian YT (2004) Large-scale growth of porous CuInS₂ microspheres. *Inorg Chem Commun* 7(4):563–565. doi:10.1016/j.inoche.2004.02.019
- Jiang Y, Qu Y, Yuan SW, Xie B, Zhang SY, Qian YT (2001) Preparation and characterization of CuInS₂ nanorods and nanotubes from an elemental solvothermal reaction. *J Mater Res* 16(10):2805–2809. doi:10.1557/Jmr.2001.0386
- Shen GZCD, Tang KB, Fang Z, Sheng J, Qian YT (2003) Polyol-mediated synthesis of porous nanocrystalline CuInS₂ foam. *J Cryst Growth* 254:75
- Shi L, Yin PQ, Wang LB, Qian YT (2012) Fabrication of single-crystalline CuInS₂ nanowires array via a diethylenetriamine-thermal route. *CrystEngComm* 14(21):7217–7221. doi:10.1039/C2ce25368b
- Baláz P (2008) Mechanochemistry in nanoscience and minerals engineering. Springer, Heidelberg
- Baláz P, Achimovičová M, Baláz M, Billik P, Cherkezova-Zheleva Z, Criado JM, Delogu F, Dutková E, Gaffet E, Gotor FJ, Kumar R, Mitov I, Rojac T, Senna M, Streletskii A, Wieczorek-Ciurowa K (2013) Hallmarks of mechanochemistry: from nanoparticles to technology. *Chem Soc Rev* 42(18):7571–7637. doi:10.1039/C3cs35468g
- Gorai S, Bhattacharya S, Liarokapis E, Lampakis D, Chaudhuri S (2005) Morphology controlled solvothermal synthesis of copper indium sulphide powder and its characterization. *Mater Lett* 59(28):3535–3538. doi:10.1016/j.matlet.2005.06.023
- Nadica D, Abazović DJJ, Stoiljković Milovan M, Mitrić Miodrag N, Ahrenkiel Scott P, Nedeljković Jovan M, Čomor Mirjana I (2012) Colloidal chemistry-based synthesis of quantized CuInS₂/Se₂ nanoparticles. *J Serb Chem Soc* 77(6):789–797
- He JJ, Zhou WH, Li M, Hou ZL, Du YF, Wu SX (2012) One-pot route for preparation of monodisperse CuInS₂ nanocrystals. *Mater Lett* 66(1):96–98. doi:10.1016/j.matlet.2011.08.013
- Katsuhiro Nose NF, Omata Takahisa, Otsuka-Yao-Matsuo Shinya, Wataru Kato MU, Nakamura Hiroyuki, Maeda Hideaki, Hayato Kamioka AHH (2009) Photoluminescence of CuInS₂-based semiconductor quantum dots; Its origin and the effect of ZnS coating. *J Phys* 165:012028
- Landsberg PT (1991) Recombination in semiconductors. Cambridge University Press, Cambridge